Effect Of Calcination Temperature On The Synthesis Of Silicon Carbide From Rice Husk With Magnesium Additive

Kieu Do Trung Kien[1,2*] and Huynh Ngoc Minh[1,2]

[1] *Faculty of Materials Technology, Ho Chi Minh City University of Technology (HCMUT), 268 Ly Thuong Kiet Street, Dien Hong Ward, Ho Chi Minh City, Vietnam*
[2] *Vietnam National University Ho Chi Minh City, Linh Trung Ward, Ho Chi Minh City, Vietnam*
[*] *Corresponding author. E-mail: kieudotrungkien@hcmut.edu.vn*

Received: Feb. 15, 2026; Accepted: Apr. 14, 2026

Silicon carbide is an advanced ceramic material widely used in structural and electronic applications due to its high thermal stability, mechanical strength, and wide bandgap properties. In this study, SiC was synthesized from rice husk through a magnesium-assisted carbothermal reduction process to reduce the reaction temperature compared with conventional methods. The SiO_2 content in the precursor mixture was adjusted by incorporating synthesized silica gel, while magnesium powder was introduced as a reducing additive. The influence of calcination temperature (500-1300°C) on phase evolution, SiC formation, and microstructural development was systematically investigated. The results indicate that calcination temperature plays a crucial role in controlling SiC formation. A significant increase in the SiC yield was observed when the calcination temperature increased from 900°C (8.25wt.%) to 1100°C (18.94 wt.%), identifying 1100°C as the optimal condition within the studied range. X-ray diffraction analysis confirmed the presence of intermediate and secondary phases, including MgO, Mg_2Si, Mg_2SiO_4, and residual SiO_2 during the reaction process. Post-synthesis acid treatment effectively removed these Mg-containing compounds and unreacted silica. Consequently, the purity of the SiC product synthesized at 1100°C improved substantially from 18.94wt.% to 94.02wt.%, as further confirmed by corresponding XRD, SEM, and EDX analyses. These findings demonstrate that magnesium-assisted synthesis enables SiC formation at considerably lower temperatures than the traditional carbothermal process, offering a promising approach for energy-efficient and sustainable production of SiC from agricultural waste.

Keywords: silicon carbide, rice husk, magnesium, carbothermal reduction, calcination temperature

http://dx.doi.org/10.6180/jase.202609_32.029

1. Introduction

Silicon carbide (SiC) is recognized as one of the advanced engineering ceramic materials with significant value across various industrial fields. Owing to its combination of outstanding mechanical and chemical properties, SiC exhibits high hardness and mechanical strength, excellent wear resistance, superior thermal stability and thermal shock resistance, and chemical inertness at elevated temperatures [1]. In addition, as a wide-bandgap semiconductor, SiC can operate stably under high-temperature and high-voltage conditions [2]. Therefore, this material is widely used in abrasive materials, refractory ceramics, furnace components, heat exchangers, aerospace applications, and particularly in next-generation power electronic devices [3–5].

Conventionally, SiC is primarily produced via the Acheson process, which involves the carbothermal reduction of high-purity SiO_2 with petroleum coke [6, 7]. However, this process requires extremely high operating temperatures (above 2500°C), consumes substantial energy, and generates significant emissions of CO and CO_2 gases [8].

These limitations necessitate the development of energy-efficient, environmentally friendly synthesis methods for SiC, as well as the use of alternative raw materials [9–11].

In this context, the use of silica-rich agricultural waste as a precursor for SiC synthesis has been considered a promising approach [12]. Rice husk is an abundant by-product of the rice industry and contains a high SiO_2 content along with a considerable amount of carbon.

Notably, silica in rice husk exists in an amorphous form, with a large specific surface area and is distributed at the nanoscale, along with intrinsic carbon. This structure enhances the reactive contact area between SiO_2 and C , thereby facilitating the carbothermal reduction reaction [13, 14]. As a result, the synthesis process can proceed at lower temperatures than in mechanically mixed sand-carbon systems [15]. Furthermore, SiC synthesized from such biogenic precursors often retains a naturally porous architecture with a high specific surface area. These microstructural features make rice husk-derived SiC highly suitable for practical applications, including advanced catalyst supports [16], lightweight thermal insulation aerogels [9], and environmental remediation platforms, such as photocatalysts for CO_2 reduction [17].

In practice, the direct synthesis of SiC from rice husk still typically requires relatively high calcination temperatures ($1600 - 1800°C$) to achieve complete conversion and good crystallinity [16, 18]. To further reduce the reaction temperature, the use of metal additives with strong oxygen affinity has been investigated, among which magnesium (Mg) has shown notable effectiveness. Mg can participate in the reduction of SiO_2, forming intermediate phases such as Mg_2Si, thereby promoting the formation of SiC at lower temperatures [19],[20]. Meanwhile, the presence of molten Mg at elevated temperatures may improve reaction kinetics and crystallization behavior.

However, the addition of Mg also leads to the formation of secondary phases, including MgO, Mg_2Si, and Mg_2SiO_4. The presence of these phases may reduce the purity and affect the final product's properties. Furthermore, calcination temperature is a critical parameter that simultaneously governs SiC formation and the development of impurity phases [21, 22]. At excessively low temperatures, the reduction reaction may be incomplete; conversely, at excessively high temperatures, Mg may evaporate or undergo excessive grain growth, thereby decreasing conversion efficiency.

While the catalytic role of Mg in lowering the synthesis temperature of SiC has been documented, previous studies have primarily focused on elucidating the fundamental reaction mechanisms or evaluating the effects of additive concentration [19, 20]. However, there remains a limited quantitative understanding of how calcination temperature governs the balance between SiC formation and the evolution of specific intermediate impurity phases (such as Mg_2Si and Mg_2SiO_4) over a wide temperature range. Furthermore, a correlation between these impurities and their responses to post-synthesis acid purification has not been well established. To address this gap, this study investigates the phase and microstructural evolution of the $SiC - Mg$ system over $500 - 1300°C$. By quantitatively assessing both the as calcined products and the effectiveness of subsequent HF treatment in removing secondary phases, this work provides a practical pathway for producing high-purity SiC from agricultural waste.

2. Experimental procedures

2.1. Materials

Rice husk was collected from a local rice milling facility and used as a natural source of silica and carbon. Prior to use, the rice husk was washed with distilled water to remove mechanical impurities, then dried at $105°C$ for 24 hours. Silica gel synthesized according to the procedure reported in [23] was added to adjust the SiO_2 content in the precursor mixture. Table 1 presents the chemical compositions of the rice husk and the silica gel. High-purity commercial magnesium powder was used as the additive.

2.2. Experimental Procedure

The experimental procedure is illustrated in Fig. 1. The dried rice husk was ground and sieved to obtain a uniform particle size. The raw material mixture, consisting of rice husk, silica gel, and Mg, was weighed according to predetermined mass ratios. The mass ratio of rice husk to Mg was fixed at 1/6, and that of rice husk to silica gel was 1/1.4. The components were thoroughly mixed by mechanical grinding in an Al_2O_3 mortar to ensure homogeneous distribution of the reactive phases. After mixing, the powder mixture was pressed into 10 mm diameter, 8 mm high pellets at 2 MPa using a hydraulic press to enhance particle contact and improve reaction kinetics during calcination.

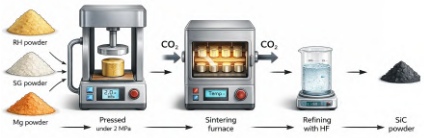

Fig. 1. Schematic of the experimental procedure for synthesizing and purifying SiC

Table 1. Chemical compositions of rice husk and silica gel

Raw materials	Si	Na	K	S	Fe	C	N	H	Others
Rice husk	6.96	0.08	0.15	0.07	0.31	45.92	3.12	6.13	35.26
Silicagel	67.20	1.75	0.12	0.06	-	-	-	-	30.87

2.2.1. From rice husk

The pellets were calcined in a resistance furnace under a CO_2 atmosphere. The calcination temperature was varied from 500 to 1300°C in increments of 200°C. This specific range was deliberately selected to capture the entire sequence of phase evolution: 500°C serves as a baseline to observe the initial decomposition of the rice husk precursor and early interactions, while 1300°C represents a critical threshold to evaluate the maximum extent of SiC formation at reduced temperatures compared to the conventional Acheson process ($>$ 1500°C). Additionally, given that the boiling point of Mg is approximately 1090°C, this upper limit allows for the assessment of reaction dynamics involving vaporized Mg. The 200°C interval was designed to provide distinct, observable stages of intermediate phase formation (e.g., Mg_2Si) and subsequent SiC crystallization without redundant experimental steps. The heating rate (10°C/ minute) and holding time (60 minutes) were kept constant for all samples to ensure comparability among experimental conditions. After calcination, the furnace was cooled to 800°C under a CO_2 atmosphere. At 800°C, the samples were held for 60 minutes in air to remove free carbon. Subsequently, the furnace was allowed to cool naturally to room temperature.

The calcined products were treated with a diluted HF solution (10%) to remove silic acontaining phases and related impurities. The acid treatment was conducted at room temperature for a duration of 30 minutes under continuous magnetic stirring at 400rpm . After treatment, the samples were washed repeatedly with distilled water until the pH reached neutrality, then dried prior to further characterization.

The SiC content and impurity phases in the as-calcined and acid-treated products were determined to evaluate the effectiveness of the calcination and purification processes.

2.3. Analysis Methods

2.3.1. SiC, SiO_2, and free carbon contents

The contents of SiC, SiO_2, and free carbon in the samples before and after purification were determined in accordance with ISO 21068-2:2008. To determine the total carbon content, the sample was combusted entirely in a tubular furnace at 1050°C, using tin powder to ensure complete oxidation and convert all carbon to CO_2 gas. For the determination of free carbon, the sample was treated with a chromic-sulfuric-iodic acid system at $130-140$°C, which selectively oxidizes the free carbon phase to CO_2. The CO_2 generated in both determinations was passed through a NaOH solution for complete absorption. The increase in mass of the absorption solution was used to calculate the carbon content according to Eq. (1) and Eq. (2). Based on the difference between total carbon and free carbon, the SiC content in the sample was calculated using the stoichiometric conversion factor presented in Eq. (3).

$$\%C_{total} = 0.2729 \times (\Delta m / m_{01}) \times 100\% \quad (1)$$

$$\%C_{free} = 0.2729 \times (\Delta m / m_{02}) \times 100\% \quad (2)$$

$$\%SiC = 3.3383 \times (\%C_{total} - \%C_{free}) \quad (3)$$

In these equations, Δm represents the increase in mass of the NaOH solution due to CO_2 absorption (g); m_{01} and m_{02} are the initial sample masses used for the determination of total carbon and free carbon, respectively (g). The factor 0.2729 is used to convert CO_2 to the corresponding carbon content, while the factor 3.3383 reflects the stoichiometric relationship between bonded carbon and SiC in the compound structure.

The SiO_2 content was evaluated through dissolution using hydrofluoric acid. The reaction mechanism is described by Eq. (4) and Eq. (5).

$$SiO_2 + 2KF + 4HF \rightarrow K_2SiF_6 + 2H_2O \quad (4)$$

$$K_2SiF_6 + 4NaOH \rightarrow 2KF + 4NaF + SiO_2 + 2H_2O \quad (5)$$

2.3.2. X-ray Diffraction (XRD)

The crystalline phase structure of the products was analyzed by X-ray diffraction (XRD) using an EMPYREAN diffractometer (PANalytical) with CuKα radiation. Diffraction data were collected over a 2θ range of 15° to 70° with a step size of 0.02°. The obtained patterns were used for phase identification and to evaluate SiC formation as a function of calcination temperature.

2.3.3. *Scanning Electron Microscopy / Energy-Dispersive X-ray Spectroscopy (SEM/EDX)*

The surface morphology and approximate elemental composition of the samples were characterized by SEM using a JSM-IT200 (JEOL) system equipped with an EDX analyzer. Micrographs were recorded at a magnification of 500×, an accelerating voltage of 10 kV, a working distance of 10.8 mm, and in secondary electron (SE) mode.

3. Results and discussion

Fig. 2 presents the SiC content of the as-calcined samples, determined in accordance with the international standard ISO 21068-2:2008. The results indicate that calcination temperature plays a decisive role in determining the formation of SiC , with a stepwise increase as temperature rises.

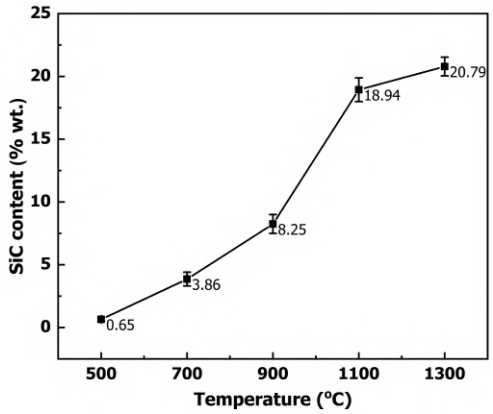

Fig. 2. Content of SiC in the as-calcined samples at various temperatures

Specifically, in the temperature range from 500°C to 900°C, the SiC content increases only gradually, reflecting the initial stage of the carbothermal reduction process. In this region, silica derived from rice husk and silica gel is not fully reduced, as the supplied thermal energy is insufficient to break the strong $Si-O$ bonds within the porous, nanostructured biogenic silica. When the temperature increases to $900-1100$°C, the SiC content rises more markedly. This enhancement can be attributed to the pronounced activation of the Mg additive, which promotes the formation of SiC and accelerates the overall reaction kinetics. From 1100°C to 1300°C, the increase in SiC content slows and gradually approaches a steady state. This behavior may be explained by a dynamic balance between the SiC formation process and the reverse oxidation reaction, as described in Eq. (6).

$$SiC + O_2 \rightarrow SiO_2 + CO_2 \tag{6}$$

At lower temperatures, the relatively low SiC content is primarily governed by direct phase competition. Thermodynamically, highly reactive Mg preferentially interacts with SiO_2 and available oxygen, leading to the predominant formation of intermediate and secondary phases such as MgO and Mg_2Si. These competing reactions involve lower activation energy barriers than the carbothermal reduction process, effectively "trapping" the reactive precursor species. As a result, the formation of SiC is kinetically hindered due to the consumption of reactants by these intermediate phases. Only at elevated temperatures ($\geq$ 900°C) does Mg_2Si acquire sufficient thermal activation to react with carbon (as described in Eq. (7)), thereby overcoming phase competition and significantly promoting the crystallization of SiC.

$$Mg_2Si + 3C \rightarrow SiC + 2Mg \tag{7}$$

The temperature-dependent, stepwise trend observed in this study highlights the catalytic effect of the Mg additive. For quantitative comparison, Pereira et al. (2020) reported that, in the conventional catalyst-free synthesis of SiC from rice husk, the SiC yield remained below approximately 20wt.% even at temperatures up to 1600°C due to insufficient activation energy [24]. In contrast, the Mg-assisted process in this work achieves a comparable SiC yield of 18.94 wt.% at a substantially lower temperature of 1100°C. Furthermore, after post-calcination acid treatment, the final SiC purity reaches 94.02wt.%, indicating that reducing the synthesis temperature does not compromise the final product quality. These quantitative comparisons clearly demonstrate that optimizing calcination temperature in the presence of Mg is critical for achieving high conversion efficiency while minimizing unnecessary energy consumption, particularly for potential industrial-scale applications. To further elucidate the temperatur edependent evolution of SiC formation, XRD was used to analyze the crystalline phase, and the results are presented in Fig. 3.

The XRD patterns reveal the presence of multiple phases, including Mg (JCPDS No. 35-0821) [25], MgO (JCPDS No. 45-0946) [26], SiO_2 in the cristobalite form (JCPDS No. 39-1425) [27], Mg_2Si (JCPDS No. 35-0773) [28], Mg_2SiO_4 (JCPDS No. 34-0189) [29], β-SiC (JCPDS No. 29-1131) [30], and α-SiC (JCPDS No. 29-1129) [31]. The presence of these characteristic diffraction peaks confirms the formation of SiC and simultaneously highlights the significant influence of temperature on phase evolution.

With increasing temperature, the diffraction peaks corresponding to SiC become sharper and more intense, indicating an enhancement in the crystallinity of both $\alpha-SiC$ and $\beta-SiC$ polymorphs. At intermediate temperatures, β-SiC

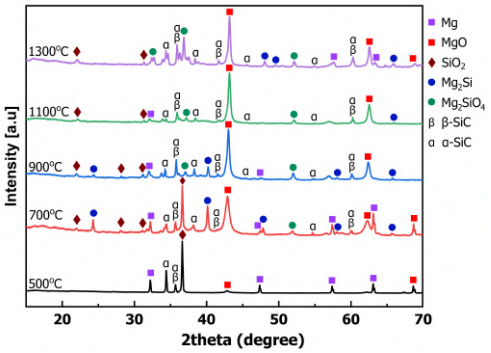

Fig. 3. XRD patterns of the as-calcined samples at various temperatures

is the dominant phase, whereas at higher temperatures, the α-SiC phase becomes more pronounced. This observation suggests that temperature not only influences the extent of SiC formation but also governs the phase transformation process between different polymorphs. Beyond the SiC polymorphs, the XRD spectra also reveal the critical role of the Mg additive through the formation of intermediate phases. According to the mechanism proposed by Jiao et al. (2020), the reaction pathway can be divided into two stages [31]. The first stage involves the reaction between Mg and SiO_2 to form Mg_2Si, as described in Eq. (8) and Eq. (9).

$$2Mg + SiO_2 \rightarrow Si + 2MgO \tag{8}$$

$$Si + 2Mg \rightarrow Mg_2Si \tag{9}$$

In this stage, Mg acts as a reducing agent, disrupting the amorphous structure of biogenic SiO_2 derived from rice husk, thereby releasing elemental Si or forming the intermediate phase Mg_2Si. In the subsequent stage, Mg_2Si and/or Si further react with carbon generated from the thermal decomposition of rice husk, as described by Eq. (7) and Eq. (10).

$$Si + C \rightarrow SiC \tag{10}$$

The presence of Mg_2Si in the XRD patterns at intermediate temperatures indicates that this phase has not fully reacted with carbon. This observation supports a two-stage, intermediate-mediated pathway, in which Mg_2Si functions as a key thermodynamic intermediate rather than SiC forming directly from SiO_2 reduction. This mechanism is consistent with those reported by Li et al. [19] and Fuad et al. [20] for Mg-assisted systems. The applicability of this mechanism to a biogenic silica precursor further confirms the model proposed by Jiao et al. [31]. In addition, this finding suggests that, in addition to temperature, other parameters, such as holding time and Mg content, may also play important roles in determining overall conversion efficiency. Furthermore, the MgO phase observed in the XRD patterns may form either through direct oxidation of Mg or via its reaction with residual SiO_2. At higher temperatures, Mg_2SiO_4 is formed, as described by Eq. (12) and Eq. (13).

$$Mg + O_2 \rightarrow MgO \tag{12}$$

$$2MgO + SiO_2 \rightarrow Mg_2SiO_4 \tag{13}$$

These phases may adversely affect the purity and final properties of the material. Moreover, the persistence of cristobalite SiO_2 even at 1300°C indicates that the overall carbothermal reduction reaction, as described by Eq. (14), has not proceeded to completion.

$$SiO_2 + 3C \rightarrow SiC + 2CO \tag{14}$$

In the absence of additives, Eq. (14) typically requires temperatures above 1470°C to proceed effectively. The presence of Mg lowers the activation energy via an intermediatemediated mechanism, thereby promoting SiC formation at lower temperatures. Notably, the detection of residual Mg at elevated temperatures may be associated with the carbothermal reduction of MgO by carbon, as described in Eq. (15).

$$MgO + C \rightarrow Mg + CO \tag{15}$$

This regenerative mechanism helps sustain catalytic activity of Mg during the high temperature calcination process. The continuous reduction of MgO by intrinsic carbon is in good agreement with the phase evolution behavior and reaction kinetics reported by Kien et al. [32] for similar agricultural waste-derived systems.

To complement the phase analysis obtained from XRD, Fig. 4 presents the quantitative contents of the main impurity phases after calcination. The results indicate that a considerable amount of free carbon remains, particularly in samples calcined at intermediate temperatures. This suggests that the carbon generated from the thermal decomposition of rice husk has not been fully consumed in the formation of SiC. One possible explanation is that the carbon particles are partially encapsulated by metallic Mg or oxide phases, thereby limiting their exposure to oxygen during the heat treatment at 800°C in air.

Similarly, the content of residual SiO_2 - qualitatively confirmed by the XRD patterns- gradually decreases with increasing calcination temperature. This declining trend indicates that SiO_2 participates more actively in the SiC formation reaction at elevated temperatures, as predicted by Eq. (14). Free carbon exhibits a comparable decreasing

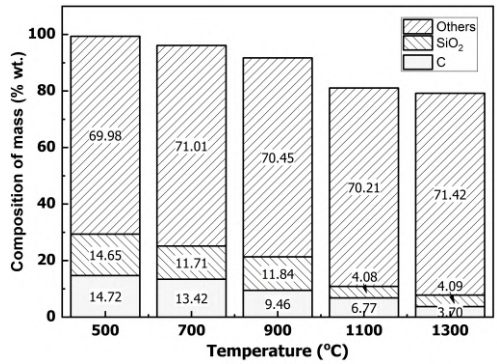

Fig. 4. Content of impurities in the as-calcined samples at different temperatures

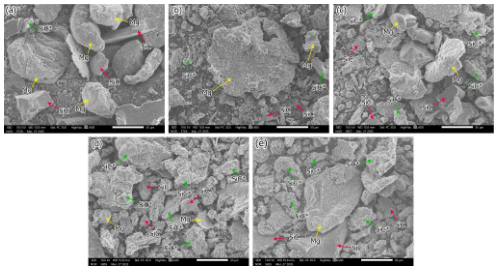

Fig. 5. SEM images of the as-calcined samples at different temperatures (Mg: $Mg/MgO/Mg_2Si/Mg_2SiO_4$; SiC: SiC ; and Si*: SiC particles surrounded by impurities). (a) 500°C, (b) 700°C, (c) 900°C, (d) 1100°C, and (e) 1300°C

tendency, while the SiC content increases correspondingly (Fig. 2), demonstrating a direct correlation between the consumption of C/SiO_2 and the formation of SiC .

The "others" fraction, representing Mg - containing compounds that were not quantitatively determined according to ISO 21068-2, remains relatively stable within the temperature range of $500 - 1300°C$. Based on the XRD results, this fraction mainly consists of Mg, MgO, Mg_2Si, and Mg_2SiO_4 - thermally stable compounds that are not fully oxidized at 800°C in air.

These findings are consistent with previous studies on SiC synthesis from rice husk, in which excess carbon at temperatures below 1500°C may reduce conversion efficiency in the absence of an appropriate catalyst.

The quantitative data presented in Fig. 4 are consistent with the results in Figures 2 and 3, further clarifying the role of temperature in controlling the balance between SiC formation and the persistence of impurity phases. To visually evaluate the influence of impurities on material morphology, the samples were examined by SEM. Fig. 5 presents the SEM micrographs of the as-calcined samples.

The SEM micrographs clearly reveal large impurity-rich regions corresponding to Mg, MgO, Mg_2Si, and Mg_2SiO_4 covering the product surface. At $500 - 700°C$, SiC particles are not significantly formed, and most of the surface is dominated by these impurity phases. At temperatures above 900°C, particles exhibiting the characteristic angular morphology of SiC begin to appear, with progressively higher density. The particle size tends to increase with calcination temperature, and the crystal morphology becomes more well-defined. Some large SiC grains are partially covered by impurity layers (denoted as SiC^*), resulting in a reduction in their sharp-edged morphology. In contrast, SiC particles with minimal impurity coverage retain a well-defined polyhedral shape, indicating potential for applications requiring high hardness and abrasion resistance.

These microstructural observations correlate with the XRD results (Fig. 3) and the quantitative impurity data (Fig. 4), indicating that the impurity phases not only exist as separate crystalline phases but also directly influence the morphological development of SiC grains. Such impurities can be chemically removed using HF treatment to enhance the purity of the final product. Fig. 6 presents the SiC content of the samples after acid treatment.

After acid treatment, the SiC content increases significantly compared with that of the untreated samples. The pronounced upward trend observed in the $900 - 1100°C$ range follows the same pattern as in Fig. 2 but with higher absolute values, indicating that the impurity phases were effectively removed through Eq. (16), Eq. (17), Eq. (18), Eq. (19) and Eq. (20).

$$Mg + 2HF \rightarrow MgF_2 + H_2 \tag{16}$$

$$MgO + 2HF \rightarrow MgF_2 + H_2O \tag{17}$$

$$SiO_2 + 4HF \rightarrow SiF_4 + 2H_2O \tag{18}$$

$$Mg_2Si + 4HF \rightarrow 2MgF_2 + SiH_4 \tag{19}$$

$$Mg_2SiO_4 + 8HF \rightarrow 2MgF_2 + SiF_4 + 4H_2O \tag{20}$$

The removal of Mg-containing and SiO_2 phases leads to an increase in the relative proportion of SiC in the final product. Fig. 7 shows a pronounced decrease in SiO_2 content after HF treatment, particularly in the $1100 - 1300°C$ temperature range. The Mg-related impurities are substantially reduced; however, a small amount of Mg_2SiO_4 remains. This phase exhibits higher chemical stability toward HF due to its stable silicate structure. Based on the experimental results, the preferential reactivity of HF toward the

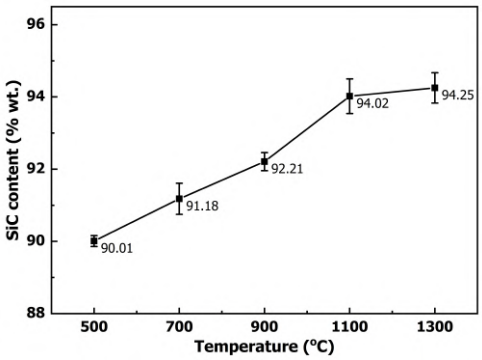

Fig. 6. Content of SiC in the samples following HF acid purification

impurity phases can be inferred, with Mg, MgO, and Mg_2Si being more readily removed than SiO_2 and Mg_2SiO_4.

The XRD patterns after acid treatment (Fig. 8) further corroborate these findings. After acid treatment, the SiC peaks become clearly dominant in the XRD patterns. SiO_2 is either present in an amorphous state or below the detection limit, particularly in the samples calcined at higher temperatures. Mg_2SiO_4 can still be observed in some high-temperature samples, consistent with the quantitative data shown in Fig. 7. To further examine morphological changes after purification, the samples were characterized by SEM (Fig. 9).

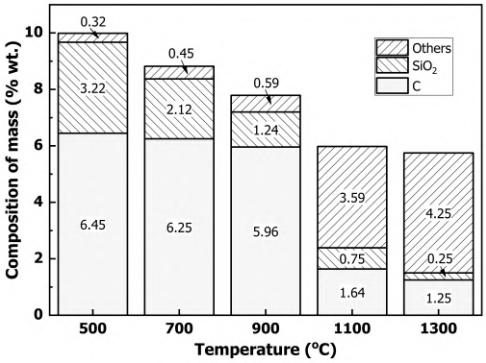

Fig. 7. Content of impurities in the samples following HF acid purification

After acid treatment, the particle surfaces become noticeably cleaner. Due to the high chemical inertness to HF at room temperature, the acid selectively removes the surrounding impurity phases without altering or degrading the SiC surface. As a result, the SiC grains are more clearly exposed, exhibiting well-defined angular morphologies and reduced secondar yphase coverage. However, in samples calcined at lower temperatures (500-900°C), remnants of the decomposed cellulose framework (RH) can still

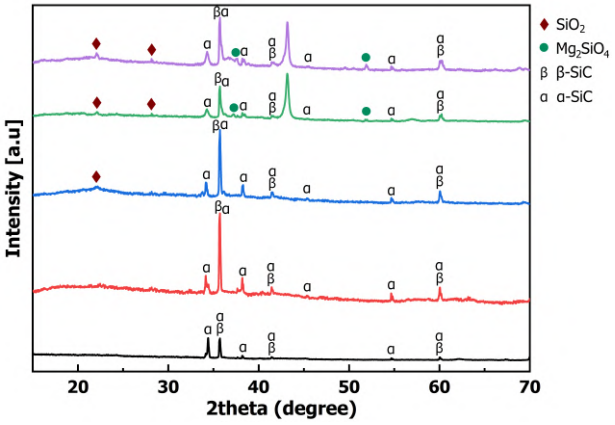

Fig. 8. XRD patterns of samples following HF acid purification

be observed, indicating that excess carbon was not fully consumed and was not completely removed during the oxidation step at 800°C. These morphological changes are consistent with the increase in SiC content after acid treatment (Fig. 6) and the corresponding reduction in impurity phases (Fig. 7). Finally, to further confirm the changes in surface composition, the elemental mapping of the samples at 1100°C are presented in Fig. 10.

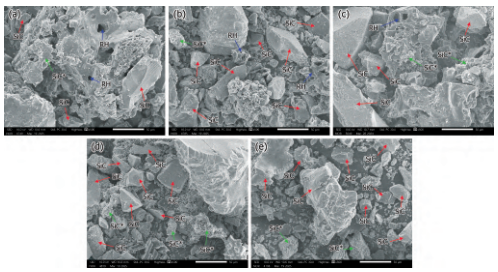

Fig. 9. SEM images of the samples following HF acid purification (Mg: **Mg**/**MgO**/Mg_2Si_2/Mg_2SiO_4; SiC: SiC and Si*: SiC particles surrounded by impurities). (a) 500°C, (b) 700°C, (c) 900°C, (d) 1100°C, and (e) 1300°C

In the untreated sample, elemental mapping reveals a heterogeneous distribution of Si and C , interspersed with regions enriched in O and Mg , indicating the presence of oxide and Mg-containing phases on the surface. After HF treatment, the distribution of Si and C becomes more uniform, while the regions associated with O and Mg are significantly reduced. This change reflects the effective removal of impurity phases and the enhancement of SiC purity. These observations are consistent with the results obtained from XRD and SEM analyses after acid treatment.

A comprehensive evaluation of the results in Fig. 2, Fig. 3, Fig. 4, Fig. 5, Fig. 6, Fig. 7, Fig. 8 and Fig. 9 indicates

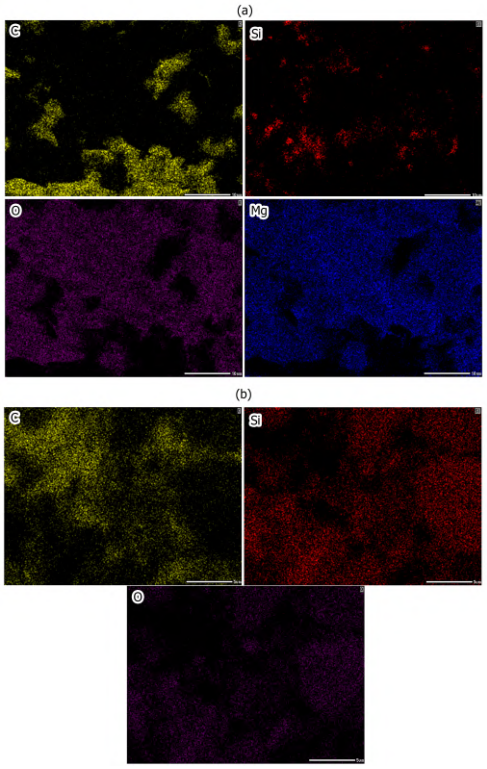

Fig. 10. The elemental distribution mapping of the samples at 1100°C before (a) and after acid treatment (b)

that 1100°C is the most suitable calcination temperature within the investigated range for SiC formation. At this temperature, a balance is achieved between SiC formation and the oxidation of the newly formed SiC . As a result, SiC is obtained with a relatively high yield and good purity after HF treatment. At the same time, the required calcination temperature of 1100°C remains significantly lower than that of conventional carbothermal synthesis methods (1500°C). This reduction in temperature has important implications for energy efficiency. According to the Stefan-Boltzmann principle, thermal radiation losses increase rapidly with temperature. Therefore, lowering the process temperature by more than 400°C can substantially reduce heat loss during the holding stage. Furthermore, from an engineering perspective, operating at 1100°C helps mitigate refractory degradation and enables the use of less capital-intensive furnace systems, thereby enhancing overall process efficiency.

While the reduction in synthesis temperature and the use of biogenic silica highlight the potential of this approach, a critical evaluation of its overall sustainability is required. The consumption of metallic Mg , which involves an energy-intensive extraction process, partially offsets the thermal energy savings achieved during calcination. In addition, the use of HF for post-synthesis purification generates fluoride-containing by-products and aqueous waste, necessitating strict and costly handling and disposal procedures. Consequently, the large-scale implementation of this batch process remains challenging. Future work should focus on developing closed-loop processing to recycle Mg -containing by-products and minimize secondary waste.

4. Conclusions

This study successfully demonstrates the synthesis of SiC from rice husk via a Mg assisted carbothermal reduction process over a temperature range of $500 - 1300$°C. An investigation of phase and microstructural evolution shows that 1100°C is the optimal temperature within the investigation range, providing an effective balance between SiC formation and secondary-phase formation while minimizing reverse oxidation. The addition of Mg acts as a catalyst, significantly reducing the required synthesis temperature compared to conventional processes. Furthermore, post-synthesis HF treatment is confirmed to be essential and highly effective, as it selectively removes intermediate by-products and cleanly exposes well-defined, highly crystalline polyhedral SiC grains, thereby improving the final product purity to 94.02wt.%. Overall, this approach represents a feasible strategy for the valorization of agricultural waste at reduced temperatures. However, to establish a truly sustainable and industrially viable production pathway, future research must address key challenges, particularly magnesium recycling and management of hazardous fluoride-containing byproducts.

5. Acknowledgements

We acknowledge the support of time and facilities from Ho Chi Minh City University of Technology (HCMUT) - VNU - HCM for this study.

References

[1] S. Ding, Y. P. Zeng, and D. Jiang, (2006) *"Thermal shock resistance of in situ reaction bonded porous silicon carbide ceramics"* **Materials Science and Engineering: A *425***(1-2): 326–329. DOI: 10.1016/j.msea.2006.03.075.

[2] G. Iannaccone, C. Sbrana, I. Morelli, and S. Strangio, (2021) *"Power electronics based on wide-bandgap semiconductors: Opportunities and challenges"* **IEEE Access *9***: 139446–139456. DOI: 10.1109/ACCESS.2021.3118897.

[3] X. Wang, X. Gao, Z. Zhang, L. Cheng, H. Ma, and W. Yang, (2021) *"Advances in modifications and high-temperature applications of silicon carbide ceramic matrix composites in aerospace: A focused review"* **Journal of the European Ceramic Society *41***(9): 4671–4688. DOI: 10.1016/j.jeurceramsoc.2021.03.051.

[4] F. L. Via, D. Alquier, F. Giannazzo, T. Kimoto, P. Neudeck, H. Ou, A. Roncaglia, S. E. Saddow, and S. Tudisco, (2023) *"Emerging SiC applications beyond power electronic devices"* **Micromachines *14***(6): 1200. DOI: 10.3390/mi14061200.

[5] T. Chun, S. Kim, J. Chung, and H. Lee, (2025) *"Numerical study on temperature and thermal stress behaviors in silicon carbide heating elements within high-temperature annealing furnaces"* **Applied Thermal Engineering *260***: 125047. DOI: 10.1016/j.applthermaleng.2024.125047.

[6] S. Jayakumari and M. Tangstad, (2020) *"Transformation of β-SiC from charcoal, coal, and petroleum coke to α-SiC at higher temperatures"* **Metallurgical and Materials Transactions B *51***(6): 2673–2688. DOI: 10.1007/s11663-020-01970-1.

[7] F. Narciso-Romero, F. Rodríguez-Reinoso, and M. Díez, (1999) *"Influence of the carbon material on the synthesis of silicon carbide"* **Carbon *37***(11): 1771–1778. DOI: 10.1016/S0008-6223(99)00045-7.

[8] V. SevastÝanov, E. P. Simonenko, A. N. Gordeev, N. P. Simonenko, A. F. Kolesnikov, E. K. Papynov, O. O. Shichalin, V. A. Avramenko, and N. T. Kuzetsov, (2013) *"Production of ultrahigh temperature composite materials* HfB_2*-SiC and the study of their behavior under the action of a dissociated air flow"* **Russian Journal of Inorganic Chemistry *58***(11): 1269–1276. DOI: 10.1134/S003602361311017X.

[9] C. Zheng, X. Li, J. Yu, Z. Huang, M. Li, X. Hu, and Y. Li, (2024) *"Biomass-derived lightweight SiC aerogels for superior thermal insulation"* **Nanoscale *16***(9): 4600–4608. DOI: 10.1039/D3NR06076D.

[10] K. D. Trung Kien and H. Ngoc Minh, (2025) *"The impact of copper additive content on the synthesis of SiC from rice husks"* **Materials Research Express *12***(2): 025502. DOI: 10.1088/2053-1591/adb12d.

[11] Y. L. Chiew and K. Y. Cheong, (2011) *"A review on the synthesis of SiC from plant-based biomasses"* **Materials Science and Engineering: B *176***(13): 951–964. DOI: 10.1016/j.mseb.2011.05.037.

[12] T. K. Kieu Do, C. T. Nguyen, and N. M. Huynh, (2024) *"Effect of temperature on the ability to synthesize SiC from rice husks"* **Materials Research Express *11***(5): 055510. DOI: 10.1088/2053-1591/ad4981.

[13] I. Hamidu, B. Afotey, B. Kwakye-Awuah, and D. A. Anang, (2025) *"Synthesis of silica and silicon from rice husk feedstock: A review"* **Heliyon *11***(4): e42491. DOI: 10.1016/j.heliyon.2025.e42491.

[14] K. D. T. Kien, H. O. Dieu, K. N. H. Thien, and M. H. Ngoc, (2023) *"Effect of rice husk morphology on the ability to synthesize silicon carbide by pyrolysis method"* **Vietnam Journal of Science and Technology *63***(5): 916–923. DOI: 10.15625/2525-2518/18511.

[15] T. Van Khai, H. N. Minh, N. V. U. Nhi, and K. D. T. Kien, (2021) *"Effect of composition on the ability to form* SiC/SiO_2*-C composite from rice husk and silica gel"* **Journal of Ceramic Processing Research *22***(2): 246–251. DOI: 10.36410/jcpr.2021.22.2.246.

[16] G. Tuci, Y. Liu, A. Rossin, X. Guo, C. Pham, G. Giambastiani, and P. H. Cuong, (2021) *"Porous silicon carbide (SiC): a chance for improving catalysts or just another active phase carrier"* **Chemical Reviews *121***(17): 10559–10665. DOI: 10.1021/acs.chemrev.1c00269.

[17] N. Xu, T. Wu, and H. Lv, (2025) *"Electrochemical conversion of rice husk in molten salts to photocatalyst for* CO_2 *photoreduction"* **Functional Materials Letters *18***(02): 2550006. DOI: 10.1142/S1793604725500067.

[18] Q. Cong, X. Zhu, Z. Ban, J. Li, Z. Cai, and L. Pei, (2025) *"Silicon Carbide-based Materials from Rice Husk"* **Current Nanoscience *21***(4): 585–595. DOI: 10.2174/0115734137316974240620095136.

[19] J. Li, X. Ren, Y. Zhang, and H. Hou, (2021) *"The role of* Mg_2Si *additive in sintering silicon carbide"* **Materials Characterization *171***: 110809. DOI: 10.1016/j.matchar.2020.110809.

[20] A. Fuad, U. Kultsum, and A. Taufiq, (2019) *"Low-temperature synthesis of α-SiC (6H SiC) nanoparticles with magnesium catalyst"* **Materials Today: Proceedings *17***(4): 1451–1457. DOI: 10.1016/j.matpr.2019.06.167.

[21] Y. Wang, X. Hou, W. Xu, and M. Tian, (2015) *"Effects of reaction temperature on the synthesis of high purity silicon carbide powder"* **Materials Research Innovations *19***(sup5): S5-1338–S5-1343. DOI: 10.1179/1432891714Z.0000000001306.

[22] K. D. T. Kien and N. V. U. Nhi, (2025) *"Effect of* Mg/Cu *additives on the ability to synthesize SiC from rice husk"* **Journal of Applied Science and Engineering** ***28***(8): 1717–1726. DOI: 10.6180/jase.202508_28(8).0009.

[23] V. H. Le, C. N. H. Thuc, and H. H. Thuc, (2013) *"Synthesis of silica nanoparticles from Vietnamese rice husk by sol-gel method"* **Nanoscale Research Letters** ***8***(1): 58. DOI: 10.1186/1556-276X-8-58.

[24] M. Pereira, D. S. D. S. Figueira, B. R. Girolamo, and F. Vernilli, (2020) *"Synthesis of silicon carbide from rice husk"* **Cerâmica** ***66***(379): 256–261. DOI: 10.1590/03666913202066379289 2.

[25] Y. Wang, Z. Gu, Y. Xin, N. Yuan, and J. Ding, (2018) *"Facile formation of superhydrophobic nickel coating on magnesium alloy with improved corrosion resistance"* **Colloids and Surfaces A: Physicochemical and Engineering Aspects** ***538***: 500–505. DOI: 10.1016/j.colsurfa.2017.11.055.

[26] L. Zhang, W. Zhu, H. Zhang, S. Bi, and Q. Zhang, (2014) *"Hydrothermal-thermal conversion synthesis of hierarchical porous MgO microrods as efficient adsorbents for lead (II) and chromium (VI) removal"* **RSC Advances** ***4***(58): 30542–30550. DOI: 10.1039/C4RA03971H.

[27] M. Hojamberdiev, A. Eminov, and Y. Xu, (2011) *"Utilization of muscovite granite waste in the manufacture of ceramic tiles"* **Ceramics International** ***37***(3): 871–876. DOI: 10.1016/j.ceramint.2010.10.032.

[28] J. Liang, X. Li, Z. Hou, C. Guo, Y. Zhu, and Y. Qian, (2015) *"Nanoporous silicon prepared through air-oxidation demagnesiation of* Mg_2Si *and properties of its lithium ion batteries"* **Chemical Communications** ***51***(33): 7230–7233. DOI: 10.1039/C5CC01659B.

[29] M. D. Alba, M. A. Castro, M. Naranjo, and E. Pavón, (2006) *"Hydrothermal reactivity of Na-n-micas (n=2,3,4)"* **Chemistry of Materials** ***18***(12): 2867–2872. DOI: 10.1021/cm0514802.

[30] D. Wu, P. Wu, Z. Xia, X. Hong, B. Qian, and P. K. Chu, (2025) *"SiC-induced modification of* $MnCo_2O_4$ *nanoneedles fabricated on Ni foam for binder-free electrodes in high-performance asymmetrical supercapacitors"* **Materials Letters** ***379***: 137665. DOI: 10.1016/j.matlet.2024.137665.

[31] Y. Jiao, J. Zhu, X. Li, F. Wang, X. Zhao, C. Shi, W. Abdul, and B. Lu, (2020) *"In-situ synthesis, microstructure and mechanism of SiC/Al-Mg-Si composites: Effects of Mg addition"* **Ceramics International** ***46***(11): 17675–17683. DOI: 10.1016/j.ceramint.2020.04.070.

[32] K. Kien and N. Nhi, (2025) *"The influence of the magnesium additive concentration on the synthesis of silicon carbide from rice husks"* **Ceramics Silikáty** ***69***(1): 63–74. DOI: 10.13168/cs.2024.0066.